

Parallels of Craniofacial Maldevelopment in Down Syndrome and Ts65Dn Mice

JOAN T. RICHTSMEIER,^{1*} LAURA L. BAXTER,² AND ROGER H. REEVES²

¹Department of Cell Biology and Anatomy, The Johns Hopkins University School of Medicine, Baltimore, Maryland

²Department of Physiology, The Johns Hopkins University School of Medicine, Baltimore, Maryland

ABSTRACT Mouse genetic models can be used to dissect molecular mechanisms that result in human disease. This approach requires detection and demonstration of compelling parallels between phenotypes in mouse and human. Ts65Dn mice are at dosage imbalance for many of the same genes duplicated in trisomy 21 or Down syndrome (DS), the most common live-born human aneuploidy. Analysis of the craniofacial skeleton of Ts65Dn mice using three-dimensional morphometric methods demonstrates an absolute correspondence between Ts65Dn and DS craniofacial dysmorphology, a distinctive and completely penetrant DS phenotype. The genes at dosage imbalance in Ts65Dn are localized to a small region of mouse chromosome 16 and, by comparative mapping, to the corresponding region of human Chromosome 21, providing independent experimental data supporting the contribution of genes in this region to this characteristic DS phenotype. This analysis establishes precise parallels in human and mouse skull phenotypes resulting from dosage imbalance for the same genes, revealing strong conservation of the evolved developmental genetic program that underlies mammalian skull morphology and validating the use of this mouse model in the analysis of this important DS phenotype. This evolutionary conservation further establishes the mouse as a valid model for a wide range of syndromes producing craniofacial maldevelopment. *Dev Dyn* 2000;217:137-145.

© 2000 Wiley-Liss, Inc.

Key words: aneuploidy; morphometrics; skull development; evolution; euclidean distance matrix analysis; segmental trisomy

INTRODUCTION

The vertebrate skull is an intricately designed, evolutionarily ancient structure. Paleontological evidence shows an evolutionary trend towards a reduction in the number of independent bony elements in more derived forms, but variation in patterns of loss, gain, or fusion of once independent cranial elements are simply embellishments on a very ancient plan (Gregory, 1963; Hanken and Hall, 1993; Moore, 1981). Within mam-

mals, the overall shape of the skull and its individual components varies from species to species. However, even among taxa as phylogenetically distinct as Rodents and Primates, correspondence of skull elements and of overall form shows that a mechanism for the conservation of cranial morphology operates across divergent mammalian taxa (Fig. 1).

Many genes are conserved across mammals, and the proximate functions of most of those genes are likely to be conserved, as well. The latent capacity of genetically-regulated developmental systems is substantiated by the occurrence of atavisms, be they true reappearances of ancestral features (Alberch, 1983) or simply variants maintained at low frequencies (Hanken and Hall, 1993), and also by experiments that produce evolutionarily lost tissues in extant organisms (Kollar and Fisher, 1980). Tissue ablation and grafting experiments illustrate patterns of derivation of the various bony elements from mesoderm, neural crest, or a combination of the two, and a growing body of evidence indicates that some of these patterns are consistent across the vertebrates (e.g., the rostro-caudal patterning of head neural crest (Langille and Hall, 1993). Conservation of the patterns of development of complex structures implies that the genetic programs that specify phenotype may also be conserved. If this were true, then recreation of a complex genetic insult with known phenotypic consequences in human would be expected to have an analogous effect in an animal model. This conservation of phenotypic endpoints would support a closer study of developmental mechanisms, and validate the animal as a model of the genetic insult in humans.

Down syndrome (DS) is a prevalent complex genetic disorder, the most frequent live-born autosomal aneuploidy in human beings. DS results from trisomy of human chromosome (Chr) 21 (Fig. 2), producing dosage imbalance for several hundred genes and resulting in a characteristic spectrum of developmental anomalies affecting many tissues (Epstein et al., 1991). Individuals

Grant sponsor: Public Health Service; Grant numbers: F33DE05706 and HD24605.

*Correspondence to: Joan T. Richtsmeier, Ph.D., Department of Cell Biology and Anatomy, The Johns Hopkins University School of Medicine, 725 N. Wolfe Street, Baltimore, MD 21205.
E-mail: jtr@mail.jhmi.edu

Received 5 August 1999; Accepted 21 October 1999

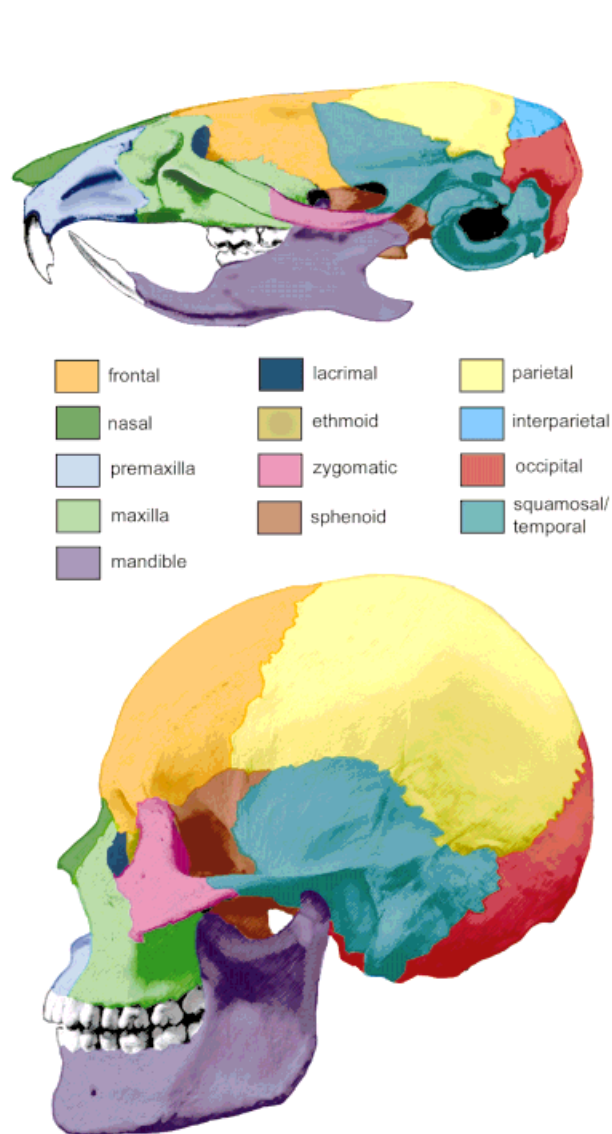


Fig. 1. Individual bony elements are conserved between mouse (**top**) and human (**bottom**) skulls. Color-coding shows correspondence of structures between the species. The interparietal bone (bright blue on the mouse skull) is an example of a skull bone that exists in the more primitive (mouse) form, but not in the more derived human skull.

with Trisomy 21 express different subsets of phenotypes that characterize the syndrome, but some DS traits occur in all DS individuals. These traits must result directly from dosage imbalance of genes on Chr21 regardless of Chr21 haplotypes, genetic background, or stochastic events. One of these completely penetrant features is the characteristic DS facies, largely a product of the underlying craniofacial skeleton. Quantitative descriptions of the characteristic features of the DS face and neurocranium are well established (Table 1).

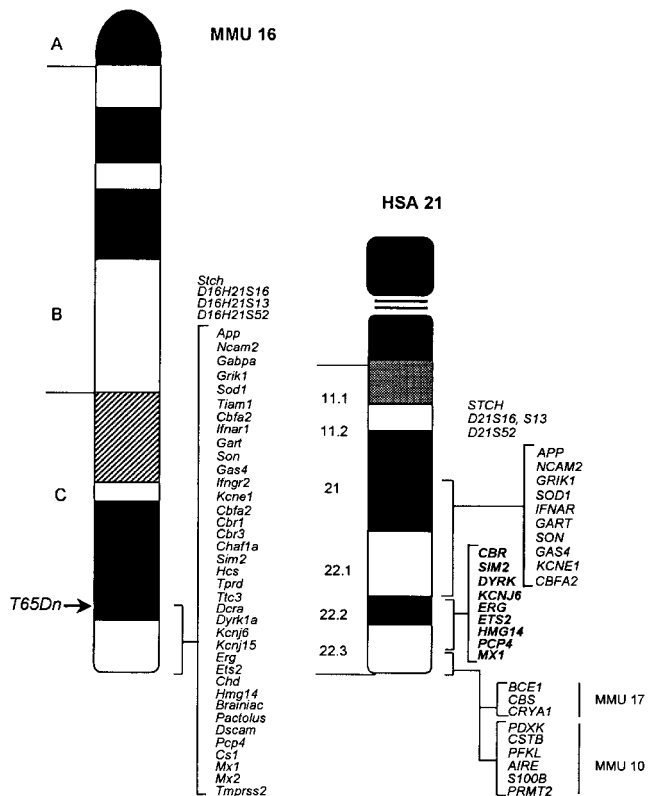


Fig. 2. Mouse Chr 16 and human Chr 21 show perfect conserved linkage for most of the long arm of Chr21, defined by 41 genes mapped to the corresponding positions in both species. All genes shared between Chr 16 and Chr 21 (Reeves and Cabin, 1999) are shown adjacent to the mouse chromosome, while a subset of corresponding human loci are shown for clarity. The cytological position of the T65Dn breakpoint on Chr16 is indicated (arrow), and the thirty-seven genes that define the region at dosage imbalance in Ts65Dn mice are included in the bracket. Genes on distal human Chr 21q22.3 are found in mouse on Chr 17 and 10. Chr 21 genes (and corresponding mouse genes) in the region from *CBR* to *MX1* have been implicated with craniofacial defects in DS (Delabar et al., 1993; Korenberg et al., 1994).

We asked whether a conserved phenotypic response could arise from a similar complex genetic insult in humans and mice using the Ts65Dn mouse, a model for DS. Distal mouse Chr16 demonstrates conserved linkage with most of human Chr21, from *STCH*, the most proximal known gene on Chr21q, to *TMPRSS2*, located in the proximal half of 21q22.3 (Reeves et al., 1998) (Fig. 2). The Ts65Dn mouse is at dosage imbalance for most of this segment (Reeves et al., 1995). These mice demonstrate several phenotypic characteristics similar to those of DS (Kola and Hertzog, 1998). In this study, analogous effects on craniofacial structure resulting from a similar complex genetic insult are shown to occur in Ts65Dn mice and DS. This supports the hypothesis that the developmental genetic pathways of skull development are conserved across mammalian taxa.

TABLE 1. Quantitative Craniofacial Phenotypes in DS and Corresponding Changes in Ts65Dn Mice

Comparison of DS craniofacial phenotype and euploid human (Reference)	Subsets of landmarks analyzed by EDMA demonstrating a corresponding difference in Ts65Dn crania
Overall reduction in head dimensions, microcephaly (Farkas et al., 1991; Fink et al., 1975; Frostad et al., 1971; Kolar and Salter, 1997; Thelander and Pryor, 1966)	Landmarks 2, 3, 4, 5, 12, 16, 23, 27; $P = 0.01$ Landmarks 3, 4, 5, 15, 16, 26, 27; $P = 0.01$
Small midface (spanning orbits and maxillary alveolus); reduced facial height (Farkas et al., 1985; Fink et al., 1975; Frostad et al., 1971; Joseph et al., 1970; Kisling, 1966; O'Riordan and Walker, 1978; Thelander and Pryor, 1966)	Landmarks 7, 10, 13, 18, 21, 24; $P = 0.030$ Landmarks 1, 3, 7, 8, 13, 18, 19, 24; $P = 0.059$
Orbital region reduced mediolaterally; reduced bizygomatic breadth (Farkas et al., 1985; Farkas et al., 1991; Joseph et al., 1970; Kisling, 1966; Kolar and Salter, 1997)	Landmarks 9, 10, 11, 14, 20, 21, 25; $P = 0.02$ Landmarks 11, 14, 22, 25; $P = 0.02$
Small maxilla (Allanson et al., 1993; Fischer-Brandies, 1988; Kisling, 1966)	Landmarks 8, 9, 10, 11, 13, 19, 20, 21, 22, 24; $P = 0.059$ Landmarks 8, 9, 10, 11, 13; $P = 0.010$ Landmarks 19, 20, 21, 22, 24; $P = 0.015$
Brachycephaly (relatively wide neurocranium) (Allanson et al., 1993; Farkas et al., 1985; Joseph et al., 1970; Kolar and Salter, 1997; Pryor and Thelander, 1967; Thelander and Pryor, 1966)	Reduction in most head dimensions but not in mediolateral dimensions (e.g., distances between landmarks 3 & 12, 3 & 16, 15 & 26, and 12 & 23) producing a broad, short (brachycephalic) skull.
Small mandible (Allanson et al., 1993; Farkas et al., 1985; Fink et al., 1975; Kisling, 1966; O'Riordan and Walker, 1978)	Distances reduced among all mandibular landmark subsets; $P \leq 0.05$ (see Fig. 3B)
Increased individual variability (Cronk and Reed, 1981; Frostad et al., 1971; Kisling, 1966; Thelander and Pryor, 1966)	Increased individual variability in mandible (See Fig. 5)

RESULTS

Twelve Ts65Dn adult mice (7 ♀, 5 ♂) and 21 euploid littermates (13 ♀, 8 ♂) were skeletonized for morphometric analysis. Three-dimensional coordinate locations of 27 cranial and 22 mandibular (Fig. 3) landmarks were recorded using the Reflex microscope. These data were analyzed using Euclidean Distance Matrix Analysis (EDMA) to measure differences in form between the sample groups (see Methods). Statistical tests of the null hypothesis of equality of shapes for subsets of landmarks (reported as P -values) and confidence interval testing for statistical evaluation of individual linear distances (using an α level of 0.10 with lower and upper confidence limits) are reported.

Confidence intervals for the direct comparison of Ts65Dn and euploid crania using the complete set of landmarks ($K = 27$) showed more than 65% of the linear distances to be significantly different between the two samples (Fig. 4). Most of these were significantly smaller in the Ts65Dn mice but varied in the magnitude of the difference. Further data exploration and statistical testing were conducted using biologically relevant landmark subsets (where $K <$ sample size), which were then compared to the results of published quantitative analyses of the DS craniofacial skeleton (Table 1).

Face

Analysis of the nasal region (landmarks 1, 2, 6, 17; $P = 0.10$), and the nasal-premaxillae-maxillae region (landmarks 1, 2, 7, 8, 9, 10, 18, 19, 20, 21; $P = 0.267$) showed nearly all individual linear distances to be significantly

smaller in the rostral portion of the Ts65Dn face (Fig. 4), but differences in overall form did not reach statistical significance. Inspection of confidence intervals for individual linear distances shows that the Ts65Dn face is of relatively normal width local to the incisors, reduced in width across the posterior maxilla, and shortened to varying degrees in all rostro-caudal dimensions excepting across the frontal process of the maxilla (landmarks 9&10 and 20&21; Fig. 4).

The aggregate of landmarks representing the maxillae (landmarks 8, 9, 10, 11, 13, 19, 20, 21, 22, 24) found Ts65Dn to be reduced in overall size and different in shape than euploid mice (Table 1). Linear distances that measure widths between paired maxillary points (landmarks 13&24, 8&19, 10&21, 9&20) were reduced to the greatest degree in Ts65Dn (Fig. 4). A less pronounced, but still significant reduction was seen for distances along the rostro-caudal axis of the maxillae.

Linear distances oriented along the rostro-caudal and mediolateral axes were smaller in the Ts65Dn face, while the anterior neurocranium was wider in Ts65Dn (landmarks 1, 2, 3, 6, 8, 12, 17, 19, 23; $P = 0.059$) (Fig. 4). Analysis of landmarks representing the zygoma (landmarks 11, 14, 22, 25; $P = 0.02$) and the zygoma and orbits (landmarks 9, 10, 11, 14, 20, 21, 22, 25; $P = 0.02$) showed the Ts65Dn face to be generally smaller than the euploid face. This pattern of underdevelopment of the maxillae and zygoma and increased width of neurocranium in Ts65Dn closely parallels quantitative changes in the analogous structures in the DS craniofacial skeleton, resulting in a small, flattened

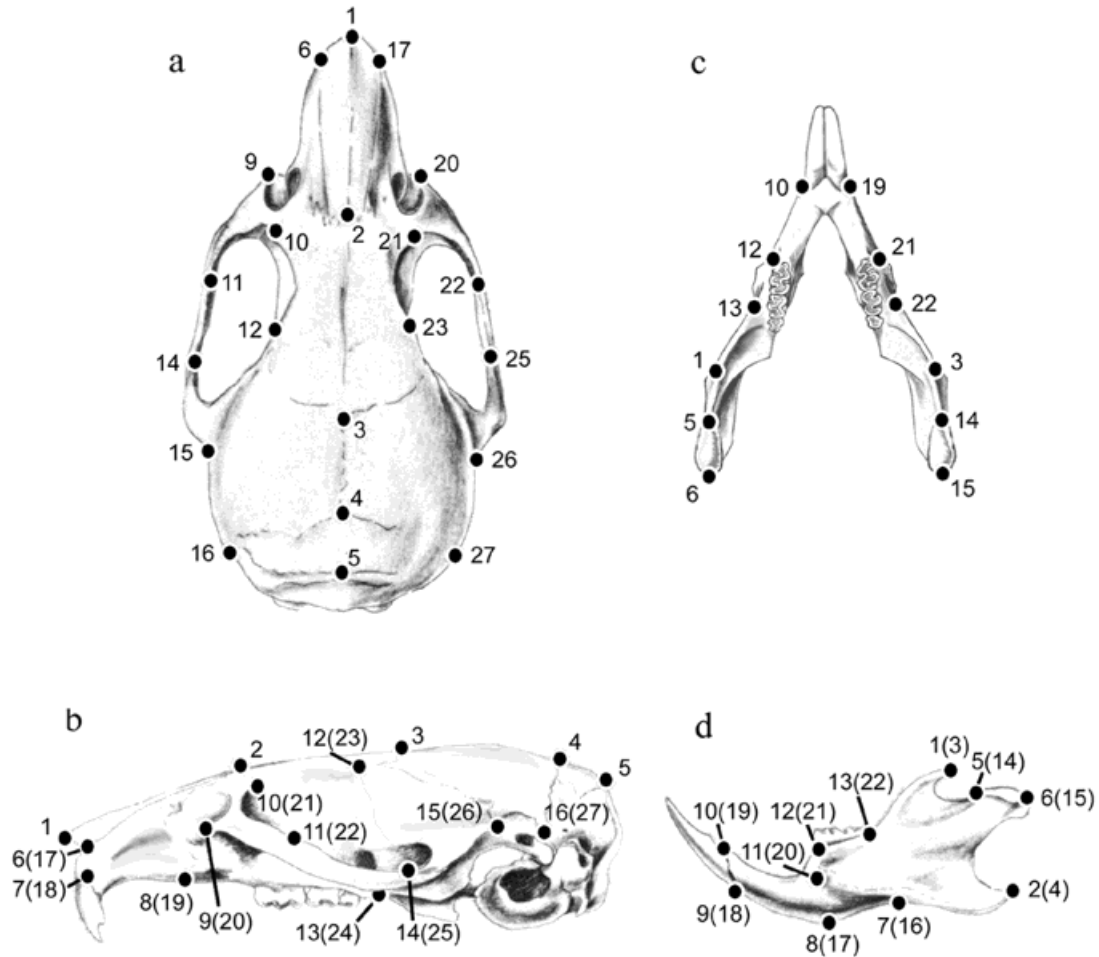


Fig. 3. Mouse skull and landmarks used in EDMA. Schematic views of the mouse cranium (a: superior view; b: lateral view) and mandible (c: superior view; d: lateral view). For bilateral landmarks, the number of the right-sided landmark is shown in parentheses. *Cranial landmarks*: (number, label) are as follows: 1, nasale; 2, nasion; 3, bregma; 4, intersection of parietal and interparietal bones; 5, intersection of interparietal and occipital bones at the midline; 6(17), anterior-most point at intersection of premaxillae and nasal bones; 7(18), center of alveolar ridge over maxillary incisor; 8(19), most inferior point on premaxilla-maxilla suture; 9(20), anterior notch on frontal process lateral to infraorbital fissure; 10(21), intersection of frontal process of maxilla with frontal and lacrimal bones; 11(22), intersection of zygomatic process of maxilla with zygoma (jugal), superior surface; 12(23), frontal-squamosal intersection at temporal crest; 13(24) intersection of maxilla and sphenoid on inferior alveolar

ridge; 14(25), intersection of zygoma (jugal) with zygomatic process of temporal, superior aspect; 15(26) joining of squamosal body to zygomatic process of squamosal; 16(27) intersection of parietal, temporal and occipital bones. *Mandibular landmarks*: 1(3), coronoid process; 2(4), mandibular angle; 5(14), anterior-most point on mandibular condyle; 6(15), posterior-most point on mandibular condyle; 7(16), superior-most point on inferior border of mandibular ramus (joining of angular notch with corpus); 8(17), inferior-most point on border of ramus inferior to incisor alveolar; 9(18), inferior-most point on incisor alveolar rim (at bone-tooth junction); 10(19), superior-most point on incisor alveolar rim (at bone-tooth junction); 11(20), mandibular foramen; 12(21), anterior point on molar alveolar rim; 13(22), intersection of molar alveolar rim and base of coronoid process.

face (Frostad et al., 1971; O’Riordan and Walker, 1978) (Table 1).

Neurocranium

The Ts65Dn neurocranium (landmarks 3, 4, 5, 12, 15, 16, 23, 26, 27; $P = 0.04$) was generally reduced in size, but confidence intervals showed that only those linear distances that span the rostro-caudal dimension were significantly smaller than in euploid mice. Linear distances along the medio-lateral axis were either the same or larger in Ts65Dn as compared to euploid. This

results in a relatively broad, or brachycephalic, Ts65Dn neurocranium, a characteristic also determined from quantitative analysis of DS individuals (Allanson et al., 1993; Thelander and Pryor, 1966).

Unlike most other medio-laterally-oriented distances on the neurocranium, the distance between landmarks 16 and 27 was reduced in the Ts65Dn mouse, and corresponds directly to the characteristic flattened occiput in DS. These osseous landmarks overlie the position of the cerebellum, which is reduced in volume in Ts65Dn and in DS (Baxter et al., 2000). The strong

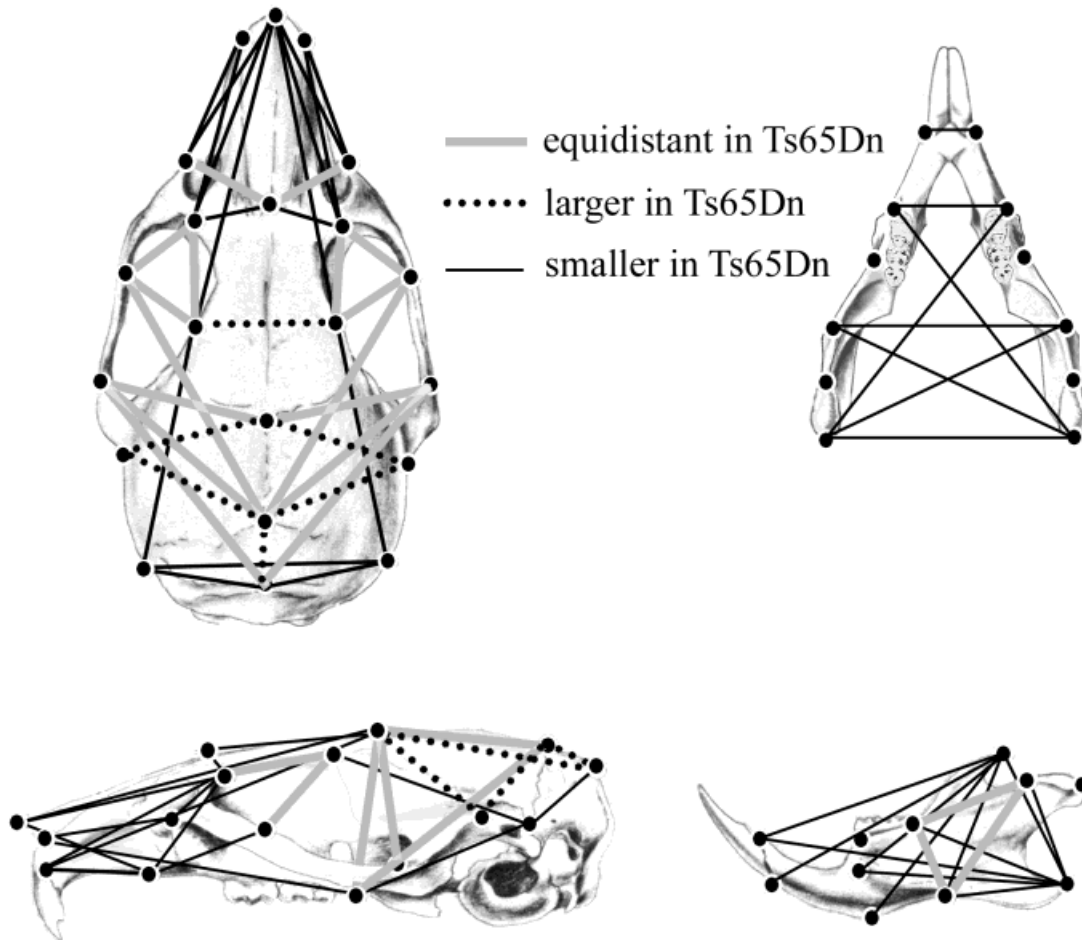


Fig. 4. Ts65Dn skulls differ significantly from euploid mice in patterns that parallel craniofacial anomalies in DS. Indicated measurements are illustrative of some of the statistically significant relationships between Ts65Dn and euploid mice.

relationship between developing brain and skull is shown by these corresponding findings in humans and mice.

Mandible

Analysis of all mandibular landmarks ($K = 22$) revealed 97% of the linear distances to be smaller in Ts65Dn mice. This was not a uniform scaling difference. Distances that were most different between Ts65Dn and euploid mice included either the coronoid process (landmarks 1,3) or the angular process (landmarks 2,4) as an endpoint, localizing the extremes of mandibular dysmorphology to these sites of muscle attachment. Reduction of the coronoid process and consequent anterior displacement of the apex of the process increased the distance between it and the condyle (landmarks 5,6,14,15), but decreased the distances between it and all other mandibular landmarks (Fig. 4). EDMA of smaller subsets of landmarks consistently found the Ts65Dn mandible to be significantly smaller than normal excepting a triangular region among three points on each hemi-mandible (land-

marks 5, 7, 13 on left, and 14, 16, 22 on right). This represents an anatomical complex that is “shape conservative” between euploid and Ts65Dn mice, and may correspond with findings in DS of a mandible that is underdeveloped but less affected than the rest of the face (Allanson et al., 1993; Fink et al., 1975; O’Riordan and Walker, 1978).

Phenotypic Variability

A model-based, data-generating algorithm (Lele and Cole, 1996) was used to compare the degree of mandible variability among individual trisomic mice relative to euploid individuals. Fifty Gaussian, random observations were generated for both the Ts65Dn and euploid mice using the sample-specific mean forms and variance-covariance matrices, which were calculated from the original three-dimensional (3D) landmark data following published methods (Lele, 1993; Lele and Cole, 1996). For Ts65Dn and euploid mice, each of the observations generated represent a landmark configuration of a hypothetical mandible based on the sample



Fig. 5. Ts65Dn mice show increased local variability of mandibular traits. Fifty Gaussian random observations were generated for each sample using the mean form and variance-covariance matrix estimated from landmarks collected on the mandibles of Ts65Dn mice (**left**) and euploid mice (**right**).

specific parameters for the mean and the variance. Two-dimensional (2D) projection of the bootstrapped left hemi-mandibles (Fig. 5) showed broader distributions around every landmark in Ts65Dn. The increased variability in the Ts65Dn mandible relative to normal corresponds with increased variability among DS individuals (Cronk and Reed, 1981; Frostad et al., 1971; Kislung, 1966; Thelander and Pryor, 1966).

DISCUSSION

Trisomy for a portion of mouse Chr16 has significant phenotypic effects on the development of the Ts65Dn craniofacial skeleton. The resulting dysmorphology closely parallels that observed in DS (Table 1), in which the same genes are at dosage imbalance. The Ts65Dn sample also exhibited increased phenotypic variability, a common finding in studies of DS characteristics. The correspondence in patterns of craniofacial dysmorphology in Ts65Dn mice and DS can be explained by the evolutionary conservation of genes regulating head development (Carroll, 1995; Davidson et al., 1995) and by similarities in the developmental processes regulating skull formation (Hanken and Hall, 1993).

The mechanisms by which aneuploidy disrupts development to produce the range of phenotypes seen in DS remain obscure. The hypothesis that a specific gene or set of genes on Chr21 can be associated with a given DS phenotype is widely accepted. This hypothesis has arisen through careful correlations of cytogenetic, molecular, and clinical manifestations in individuals with translocations resulting in trisomy for a subset of Chr21 genes (segmental trisomy 21). Maps correlating dosage imbalance of specific critical regions with specific characteristics provide useful information about segments in which to search for the genes primarily

responsible (Delabar et al., 1993; Korenberg et al., 1994). The proposed distal Chr21 boundary for genes contributing to the DS face is defined by the included marker, *MX1*, and the excluded marker, *BCEI*, which is ca. 400 kb distal (Fig. 2). The most distal gene on Chr16 is *Tmprss2*, within a few kb of *Mx1*, thus independently refining the distal boundary of genes contributing to anomalies of the craniofacial skeleton in this aneuploid syndrome.

Despite advances in correlating regions of Chr21 with DS phenotypes in individuals with segmental trisomy 21, the ultimate resolution of these maps is limited by the small number of affected individuals and by the significant phenotypic variability observed even among those with full trisomy 21. Further, the "smallest region of overlap" approach to phenotype mapping in translocation DS suffers from another, more important limitation; no individual is actually at dosage imbalance for only the common region. Therefore, this type of analysis cannot discriminate between the action of a single, dosage sensitive gene on a diploid background or on a genetic background destabilized by aneuploidy for many genes. The mapping of DS traits requires an animal model in which genetic background is relatively uniform and in which multiple individuals with the same chromosome segments at dosage imbalance can be evaluated. The occurrence of directly parallel craniofacial phenotypes in Ts65Dn mice and DS validates the use of mouse models to study the basic mechanisms producing these effects.

In our investigation of the processes by which trisomy for a given genetic region causes a constellation of features recognized as DS, we have discovered a specific genetic region in mice and in humans that causes particular craniofacial anomalies when present at dos-

age imbalance. Mutations in these same genes in euploid individuals might affect normal variability of the craniofacial complex in similar ways. Although the entire region is at dosage imbalance in the Ts65Dn mouse, overexpression of a specific gene or groups of genes in this region would enable identification of pathways of specific aspects of craniofacial maldevelopment. Chromosome engineering in mice (Ramirez-Solis et al., 1995) can be used to produce reciprocal translocations that result in precisely defined segmental trisomy, and these mice can be assessed quantitatively for any completely penetrant phenotypic endpoint of trisomy that is directly relevant to DS. Such studies can efficiently localize genes responsible for a phenotype and knowledge of the genes can provide a vehicle for understanding genetic regulation of normal development, as well as the development of anomalies associated with DS. Our results identify conserved developmental pathways between DS and the Ts65Dn mouse that validate the use of this model in efforts to define the mechanisms by which aneuploidy disrupts development.

EXPERIMENTAL PROCEDURES

Animal Husbandry

All mice were maintained in a virus and antibody-free facility with food and water ad libitum. Ts65Dn mice (B6EiC3H-a/A-Ts65Dn, Jackson Laboratory) are maintained on the B6/C3H background. Mice used in this study were generated by crossing female Ts65Dn mice with B6/C3H or CBA/CaJ mice (Jackson Laboratory). Genotypes were determined by karyotyping blood obtained from the retro-orbital sinus (Davisson et al., 1993). Only mice from litters of 4–6 offspring were used. All mice were adults ranging from 4–7 months old except for one mouse that was 12 months old. The strains of mice used do not show sexual dimorphism in cranial structure (Goffinet and Rakic, 2000). To investigate the possibility of sex dimorphism in our samples, all analyses were repeated comparing the female Ts65Dn mice to an all-female subsample of euploid littermates. Results of all single sex analyses were consistent with those presented here. All procedures were approved by the Institutional Animal Care and Use Committee.

Preparation of Skeletons and Landmark Data Collection

Mice were sacrificed and carcasses were skinned and gutted and put into a Dermestid beetle colony for cleaning. Three-dimensional locations of cranial and mandibular landmarks were recorded directly from the skeletons using the Reflex microscope. The Reflex microscope (<http://web.ukonline.co.uk/reflex/reflex.html>) represents fusion between a small coordinate measuring machine and a surface profiler, and is ideal for measuring locations, distances and angles in three dimensions on small, irregular surfaces. The object is viewed through an adapted stereoscopic microscope

where a small light spot appears in the field of view and can be moved by using the motorized stage until the relevant point on the surface of the object coincides with the spot. The Reflex Microscope uses the stereoscopic ability of the observer to find and record biologically relevant loci (landmarks) by precisely locating the tiny illuminated spot over the landmark. The X , Y , Z coordinates of the spot are monitored continuously via linear encoders. Once the spot overlies a relevant biological location, the X , Y , Z coordinates of the landmark can be stored in a computer file. A previous model of the Reflex microscope was reviewed by McLarnon (MacLarnon, 1989). Measurement error was inspected following methods outlined elsewhere (Richtsmeier et al., 1995) and minimized statistically by digitizing each specimen multiple times, and using the average of the various trials for analysis.

Morphometric Methods

Euclidean Distance Matrix Analysis (EDMA) (Lele, 1993; Lele and Richtsmeier, 1991) is a 3D morphometric technique that is invariant to the group of transformations consisting of translation, rotation, and reflection. Since the form of an object is invariant regardless of whether the form is rotated, translated, or reflected, group invariance must be maintained in the statistical analysis of forms. Original data consist of 3D coordinates of landmark locations collected from the forms under study. These are stored as $K \times 3$ matrices where K = the number of landmarks. The data are re-written and analyzed as a matrix of all unique linear distances among landmarks. This matrix is called the form matrix, or FM . The original landmark coordinate data are used to estimate a mean FM for each sample being considered following procedures outlined by Lele (Lele, 1993). Form difference between samples is evaluated by calculating ratios of like-linear distances using the mean FM s of the two samples. The matrix of ratios of like-linear distances is called the form difference matrix (FDM). If a particular linear distance is similar in two samples, that ratio will equal 1.

For reasons detailed elsewhere (Lele and McCulloch, 1999; Lele and Richtsmeier, 2000), nuisance parameters of rotation and translation prohibit valid estimates of the exact magnitude of variability local to each landmark, but the available estimates can be used for statistical testing and for visualization of the distribution of variability across an object. In our study, the landmark coordinates for the mean mandibular form and the variance-covariance matrix were used to visualize variability local to landmarks. The mean form is used as a template and the hypothetical landmark locations are constrained by the variance estimates local to each landmark and by the covariances calculated among the landmarks. The choice of coordinate system in which to project the mean form and the variance distribution around each landmark is arbitrary (see Fig. 5).

Form difference is statistically evaluated using estimates of the mean FM s and variance-covariance struc-

ture for each sample. Nonparametric statistical techniques test the null hypothesis of similarity in form between the samples to determine whether a difference in form exists, and if it does, whether it is due solely to size (scaling), or if there is a shape component ($P = 0.05$ is traditionally used as the level of significance). This nonparametric test for overall similarity in shape uses the original data to generate random samples, each containing the same number of specimens as the true sample. A *FDM* is calculated for each pair of bootstrapped samples, and a test statistic (maximum ratio of inter-landmark distances divided by minimum ratio, or *max/min*) is calculated for each pair. This is done an adequate number of times (200–300). The test compares the true *max/min* calculated from the original data to the distribution of the *max/min* values for the bootstrapped samples. If the true *max/min* lies outside of 95% of the bootstrapped *max/min* values, we reject the null hypothesis of similarity in shape (Lele and Richtsmeier, 1991). Further examination of the *FDM* identifies patterns of localized differences in form between the two samples.

To statistically test for localized differences in form, an alternate nonparametric bootstrap procedure calculates the $100(1-\alpha)\%$ confidence interval for each linear distance (for reasons presented by Lele and Richtsmeier (1995), we set $\alpha = 0.10$). If this interval contains the value 1.0, the null hypothesis of similarity for that linear distance is accepted. Confidence intervals enable the identification of those linear distances that are most similar or different between the samples. *EDMA* programs are down loadable from <http://faith.med.jhmi.edu/>.

ACKNOWLEDGMENTS

We thank William Atchley, James Cheverud, Charles Epstein, and John D. Gearhart for critical review of the manuscript, Kenneth Rose for thoughtful discussions of the evolution of mammals, and Linda Gordon of the National Museum of Natural History for preparing the skeletons. Kristina Aldridge, Jide Anikwu, and Valerie DeLeon produced the graphics. This work was supported by PHS awards F33 DE05706-02 (JTR) and HD24605 (RHR).

REFERENCES

- Alberch P. 1983. Morphological variation in the neotropical salamander genus *Bolitoglossa*. *Evolution* 37:906–919.
- Allanson J, O'Hara P, Farkas L, Nair, R. 1993. Anthropometric craniofacial pattern profiles in Down syndrome. *Am J Med Genet* 47:748–752.
- Baxter LL, Moran TH, Richtsmeier JT, Troncoso J, Reeves RH. 2000. Discovery and genetic localization of Down Syndrome cerebellar phenotypes using the Ts65Dn mouse. *Hum Mol Genet*, In press.
- Carroll S. 1995. Homeotic genes and the evolution of arthropods and chordates. *Nature* 376:479–485.
- Cronk C, Reed R. 1981. Canalization of growth in Down syndrome children three months to six years. *Hum Biol* 53:383–398.
- Davidson E, Peterson K, Cameron R. 1995. Origin of bilaterian body plans: evolution of developmental regulatory mechanisms. *Science* 270:1319–1325.
- Davisson M, Schmidt C, Reeves N, Irving E, Akeson E, Harris B, Bronson R. 1993. Segmental trisomy as a mouse model for Down Syndrome. *Prog Clin Biol Res* 384:117–133.
- Delabar J-M, Theophile D, Rahmani Z, Chettouh Z, Blouin J-L, Priet M, Noel B, Sinet P-M. 1993. Molecular mapping of twenty-four features of Down Syndrome on Chromosome 21. *Eur J Hum Genet* 1:114–124.
- Epstein CJ, Korenberg JR, Anneren G, Antonarakis SE, Ayme S, Courchesne E, Epstein LB, Fowler A, Groner Y, Huret JL, et al. 1991. Protocols to establish genotype-phenotype correlations in Down syndrome. *Am J Hum Genet* 49:207–235.
- Farkas L, Munro I, Kolar J. 1985. Abnormal measurements and disproportions in the face of Down's syndrome patients: preliminary report of an anthropometric study. *Plast Reconstr Surg* 75:159–167.
- Farkas L, Posnick J, Hreczko T. 1991. Anthropometry of the head and face in 95 Down Syndrome patients. In: Epstein C, editor. *The morphogenesis of Down Syndrome*. New York:Wiley-Liss. p 53–97.
- Fink G, Madaus W, Walker G. 1975. A quantitative study of the face in Down's syndrome. *Am J Orthod* 67:540–553.
- Fischer-Brandies H. 1988. Cephalometric comparison between children with and without Down's syndrome. *Eur J Orthodontics* 10: 255–263.
- Frostad W, Cleall J, Melosky L. 1971. Craniofacial complex in the Trisomy 21 syndrome (Down's syndrome). *Archs Oral Biol* 16:707–722.
- Goffinet A, Rakic P. 2000. *Mouse Brain Development*. Berlin: Springer, in press.
- Gregory W. 1963. *Our face from fish to man*. New York: Hafner Publishing. 295 p.
- Hanken J, Hall B. 1993. Mechanisms of skull diversity and evolution. In: Hanken J and Hall B, editors. *The Skull: functional and evolutionary mechanisms*. Chicago: University of Chicago Press. p 1–36.
- Joseph M, Dawbarn C, Healy M. 1970. *Measurement of the facies: a study in Down's Syndrome*. London: William Heinemann Medical Books, Ltd. 115 p.
- Kisling E. 1966. Cranial morphology in Down's syndrome: a comparative roentgencephalometric study in adult males. Copenhagen: Munksgaard. 107 p.
- Kola I, Hertzog P. 1998. Down syndrome and mouse models. *Curr Opin Genet Dev* 8:316–321.
- Kolar J, Salter E. 1997. *Craniofacial anthropology: Practical measurement of the head and face for clinical, surgical, and research use*. Springfield: Charles C Thomas. 334 p.
- Kollar E, Fisher C. 1980. Tooth induction in chick epithelium: expression of quiescent genes for enamel synthesis. *Science* 207:993–995.
- Korenberg J, Chen X, Schipper R, Sun Z, Gonsky R, Gerwehr S, Carpenter N, Daumer C, Dignan P, Disteche C, Graham J, Hugins L, McGillivray B, Miyazaki K, Ogasawara N, Park J, Pagon R, Puschel S, Sack G, Say B, Schuffenhauer S, Soukup S, Yamanaka T. 1994. Down syndrome phenotypes: the consequences of chromosomal imbalance. *Proc Natl Acad Sci* 91:4997–5001.
- Langille R, Hall B. 1993. Pattern formation and the neural crest. In: Hanken J, Hall B, editors. *The skull*. Chicago: University of Chicago Press. p 77–111.
- Lele S. 1993. Euclidean distance matrix analysis (EDMA) of landmarks data: estimation of mean form and mean form difference. *Math Geol* 25:573–602.
- Lele S, Richtsmeier JT. 1991. Euclidean distance matrix analysis: a coordinate free approach to comparing biological shapes using landmark data. *Am J Phys Anthropol* 86:415–428.
- Lele S, Richtsmeier JT. 1995. Estimating confidence intervals for the comparison of forms. *Am J Phys Anthropol* 98:73–86.
- Lele S, Cole TM, III. 1996. A new test for shape differences when variance-covariance matrices are unequal. *J Hum Evol* 31:193–212.
- Lele S, McCulloch C. 2000. Invariance and morphometrics. *Journal of American Statistical Association*. In press.
- Lele S, Richtsmeier J. 2000. *An invariant approach to the statistical analysis of shapes*. London: Chapman & Hall/CRC Press. In press.
- MacLarnon A. 1989. Applications of the Reflex Instruments in quantitative morphology. *Folia Primatol* 53:33–49.
- Moore W. 1981. *The mammalian skull*. Cambridge: Cambridge University Press. 369 p.

- O'Riordan M, Walker G. 1978. Dimensional and proportional characteristics of the face in Down's syndrome. *Journal of Dentistry for the Handicapped* 4:6-9.
- Pryor H, Thelander H. 1967. Growth deviations in handicapped children. *Clinical Pediatr* 6:501-512.
- Ramirez-Solis R, Liu P, Bradley A. 1995. Chromosome engineering in mice. *Nature* 378:720-724.
- Reeves RH, Cabin DE. 1999. Mouse chromosome 16. *Mamm Genome* 10:957.
- Reeves RH, Irving N, Moran T, Wohn A, Kitt C, Sisodia S, Schmidt C, Bronson R, Davisson M. 1995. A mouse model for Down syndrome exhibits learning and behavior deficits. *Nat Genet* 11:177-184.
- Reeves RH, Rue E, Yu J, Kao F-T. 1998. Stch maps to mouse Chromosome 16 extending the conserved syntenic region with human Chromosome 21. *Genomics* 49:156-157.
- Richtsmeier JT, Paik C, Elfert P, Cole III TM, Dahlman H. 1995. Precision, repeatability and validation of the localization of cranial landmarks using computed tomography scans. *Cleft Palate Craniofac J* 32:217-227.
- Thelander H, Pryor H. 1966. Abnormal patterns of growth and development in mongolism. *Clin Pediatr* 5:493-501.